Physics – Uspekhi **62** (3) 257 – 265 (2019)

FROM THE CURRENT LITERATURE PACS numbers: 33.20.Ea, 42.62.Fi, **42.65. – k**

On a half-forgotten but very powerful method for coherent spectroscopy of molecules

A A Makarov, E A Ryabov

DOI: https://doi.org/10.3367/UFNe.2018.12.038492

Contents

Abstract. The sum-frequency generation involving two infrared laser quanta and a single visible-range laser quantum is a four-wave mixing process that is virtually not used in practice. Nevertheless, this process provides an extremely high selectivity with respect to the Q-branch of the two-photon vibrational transition in molecules. We explore here two publications: one that is more than thirty years old, and another that appeared in 2018, to show broad potential applications of the method. The objective reasons why this potential has not been used so far are discussed.

Keywords: sum frequency generation, two-photon resonance, infrared spectroscopy of molecules

1. Introduction

A recently published article [1] announced the presentation of a new spectroscopic technique for attaining efficient low-background coherent Raman scattering. The title of the paper, "Two-photon infrared resonance can enhance coherent Raman scattering," clarifies the essence of the method. Its publication in *Physical Review Letters* can be regarded as a very important event in spectroscopy. On the whole, we share this opinion although emphasizing that the novelty of the method allows exaggeration, because the scheme of experiment [1] does not, in principle, differ from the generally known four-wave mixing with two intermediate resonances (quasiresonances) (see, for instance, review [2]). Nevertheless, we wish to demonstrate in the present article the uniqueness and utility for molecular spectroscopy of some variants of the approach employed in Ref. [1], including one verified long ago.

There are several four-wave processes having found application in spectroscopy and in studying various physical phenomena. Figure 1 presents energy diagrams of two such processes. One is a well-known method of coherent anti-Stokes Raman scattering (CARS) spectroscopy.[1] Its various applications are discussed in many reviews, too numerous to mention here. The other is third-harmonic generation. Some publications report application of this process for nonlinear frequency conversion [5, 6], the spectroscopy of multiphoton resonances [7], and investigations into the infrared (IR) multiphoton excitation of molecules [8]. The necessary and sufficient condition for observation of directed coherent radiation in these processes is the fulfilment of the laws of energy and momentum conservation in a medium.[2]

In the foregoing, citation was limited only to those studies of third-harmonic generation that were known by the time of publication of Ref. [12] reporting a detailed investigation of the variant of four-wave mixing, the subject matter of the present article. This variant (Fig. 2a) deals with a sum-frequency generation

$$\omega_{\rm sum} = 2\omega_{\rm ir} + \omega_{\rm vis}\,, \qquad (1)$$

where frequency $\omega_{\rm ir}$ lies in the region of the fundamental vibrational absorption band, and frequency $\omega_{\rm vis}$ is in the

A A Makarov [1,2], **E A Ryabov** [1]
[1] Institute of Spectroscopy, Russian Academy of Sciences, ul. Fizicheskaya 5, 108840 Troitsk, Moscow, Russian Federation
[2] National Research University 'Higher School of Economics', ul. Myasnitskaya 20, 101000 Moscow, Russian Federation
E-mail: amakarov@isan.troitsk.ru, ryabov@isan.troitsk.ru

Received 11 June 2018, revised 5 December 2018
Uspekhi Fizicheskikh Nauk **189** (3) 271 – 280 (2019)
DOI: https://doi.org/10.3367/UFNr.2018.12.038492
Translated by Yu V Morozov; edited by A Radzig

[1] In the very first monograph [3] that followed review [2], CARS was regarded as a variant of active Raman scattering spectroscopy (ARS) (see also the chapter written by Sergey Aleksandrovich Akhmanov in monograph [4] edited by the Nobel Prize laureate in Physics 1981 Nicolaas Bloembergen and dedicated to the memory of Rem Viktorovich Khokhlov).
[2] For completeness, it is appropriate to mention 'degenerate' schemes of four-wave mixing in which the frequency of the generated photon coincides with the frequencies of the input photons. Such schemes comprise, in particular, the photon echo [9], phase conjugation [10] and spectroscopy in separated optical fields [11].

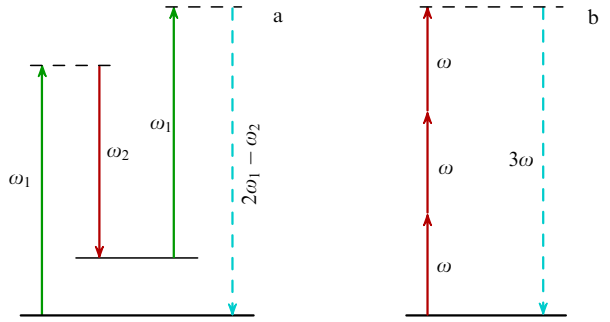

Figure 1. Two popular four-wave mixing schemes. Solid lines show acting wave frequencies, and the dashed line denotes the generated wave frequency. (a) CARS: as a rule, there is a single resonance in this process; therefore, the so-called nonresonant background may prove to be of importance (see discussion at the end of Section 2.1). CARS is employed as a variant of RS spectroscopy to measure characteristics of this resonance by tuning frequency ω_2. (b) Third-harmonic generation is most frequently used for frequency conversion; intermediate resonances (quasiresonances) are able to enhance this process.

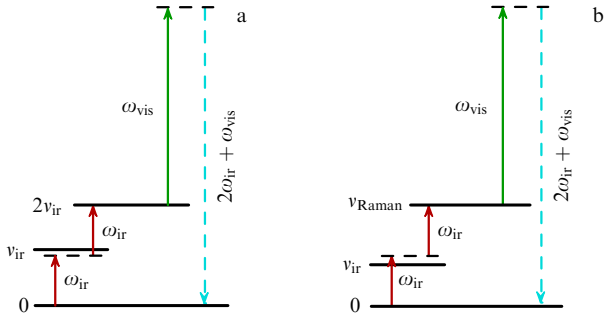

Figure 2. Two variants of two-photon molecular vibrational spectroscopy. (a) Two-photon resonance is tuned to the first overtone of the IR-active mode. Intermediate quasiresonance state is the state of the *same* mode with occupation number equal to unity. (b) Two-photon resonance is tuned to fundamental transition in the RS-active mode. The intermediate quasiresonance state may be the first excited state of *another*, IR-active, mode.

visible range. It is easy to see that third-harmonic generation (Fig. 1b) is a special case of process (1) discussed in some earlier papers. For example, Ref. [13] presents a calculation of nonlinear cubic susceptibility $\chi^{(3)}$ responsible for sum-frequency generation for the HCl molecule; Ref. [14] deals with spectroscopic aspects of the process, and Refs [15, 16] report the first experimental observations. Reference [12] discusses a more or less systematic study demonstrating and explaining very high spectral selectivity of a number of molecules with respect to the Q-branch of the two-photon transition (in comparison with that in the case of the wide PQR-structure of the single-photon absorption band). Moreover, the paper contains a theoretical prediction of the possibility of observing an abnormally narrow peak inside the Q-branch.[3]

We were unaware of any further attempts to involve this process for molecular vibrational spectroscopy[4] till the appearance of Ref. [1]. They seem to have remained equally unknown to the authors of paper [1], who cited neither studies published after 1986 nor Refs [12–15]. Formally, experiment [1] was designed to study the same process (1). However, there is a significant difference from the scheme presented in Fig. 2a, where intermediate resonance (quasiresonance) for two-photon transition was associated with the one-photon transition in the same vibrational mode of the molecule. In the new case [1] (Fig. 2b), the final state of the two-photon transition represents the singly excited state of the mode active with respect to Raman scattering (RS) (Raman-active mode), while the intermediate quasiresonance transition is related to the singly excited state of *another* (IR-active) mode having a frequency *accidentally close* to the one-photon resonance.

The difference between the schemes of processes in Refs [1, 12] is of significance from both the standpoint of implementation and spectroscopic applications. Peculiar features of these schemes are considered in Sections 2 and 3.

2. Two-photon resonance spectroscopy of infrared-active vibrational transitions of molecules

2.1 Universal properties and general patterns

Sum-frequency generation (1) is especially efficient in the case of simultaneous application of two laser pulses to a gaseous medium: one with frequency ω_{ir} in the IR range in the region of the IR-active vibrational mode of the molecule, and the other with frequency ω_{vis} in the visible range. This process was thoroughly investigated first in experiment [12] for four molecules: SF_6, BCl_3, CF_3I, and CF_3Br. The source of IR radiation was a CO_2-laser with discrete frequency tuning in the 9.6- and 10.6-μm ranges, and with the typical distance between lines in different bands and/or generation branches of 1.2–1.3 cm^{-1}. The second harmonic of an Nd:YAG laser (532 nm) served as the source of visible radiation. Because the widths of Q-branches[5] in the *linear* absorption spectra at room temperature were on the order of 1–1.5 cm^{-1}, at least one line of the CO_2-laser fell in the Q-branch region of the two-photon transition, i.e., in the state with *double* excitation of the resonance mode.[6] The experiment measured a signal at the sum frequency ω_{sum} (1); the signal abruptly increased to the maximum value when frequency ω_{ir} most closely coincided with the two-photon transition frequency:

$$\omega_{ir} \approx \frac{1}{2}\,\omega_{20} = \omega_{10} + x\,, \qquad (2)$$

where subscripts denote vibrational quantum numbers, and x is the anharmonic constant of the resonance mode (usually negative). The results of measurements are reported in Ref. [12]. They will be presented below for one of the molecules, CF_3Br, together with the calculations also made by the same authors using spectroscopic constants reliably known at that time.

In the framework of the perturbation theory, signal intensity for process (1) is expressed as

$$I_{sum} \propto I_{ir}^2 I_{vis} L^2 N^2 \left|\chi^{(3)}(-\omega_{sum}, \omega_{vis}, \omega_{ir}, \omega_{ir})\right|^2\,, \qquad (3)$$

[3] It was not realized in experiment because of the lack of a continuously turnable laser.

[4] For example, detailed review [17] published in 1999 contained no references to process (1).

[5] Q-branch is the aggregate of lines corresponding to vibrational-rotational transitions in molecules without a change of rotational quantum numbers.

[6] The two-photon resonance frequency is shifted a few wave numbers relative to the frequency of a one-photon resonance due to anharmonism.

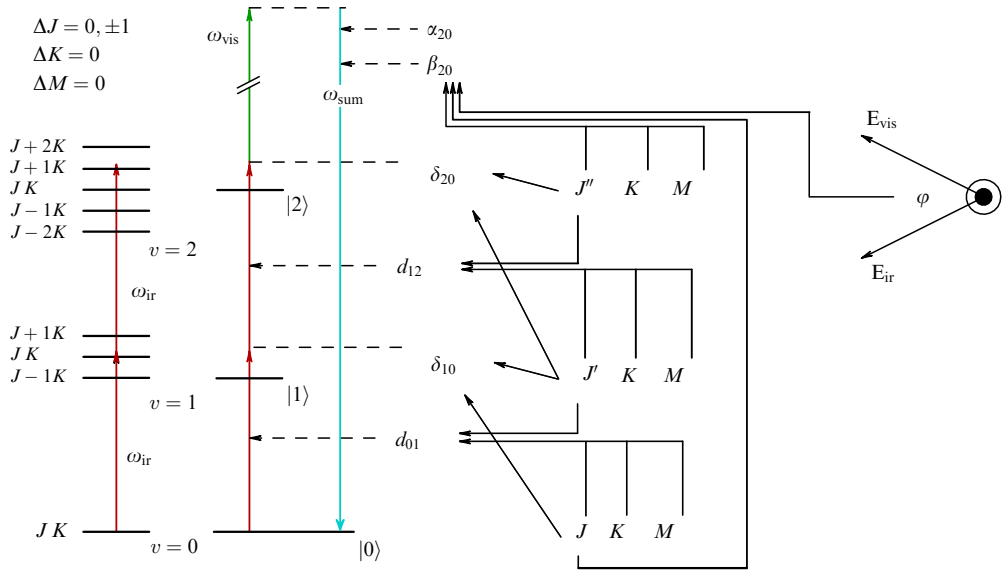

Figure 3. Channels to from Raman polarizability at the overtone of the symmetrical top molecule parallel band as a result of interaction with the IR field. All possible channels are shown on the left side of the figure. (For the initial state $|v=0\rangle$: J — total angular momentum, K — projection of J on the molecule symmetry axis. It is assumed that IR radiation is linearly polarized; M — projection of **J** on the polarization axis.) Right part of the figure shows an individual channel together with functional dependences schematically indicated by thin arrows. Notations are as follows: α_{20} — vibrational component of polarizability (tensor), β_{20} — rotational part of Raman polarizability, d_{01}, d_{12} — dipole moments, and $\delta_{10} = \omega_{ir} - \omega_{10}$, $\delta_{20} = 2\omega_{ir} - \omega_{10} - \omega_{21}$.

where I_{ir}, I_{vis} are the IR and optical radiation intensities, respectively, L is the medium length, N is the molecule concentration, and $\chi^{(3)}$ is the cubic nonlinear susceptibility in standard notations (see, for instance, Ref. [3]). Quantity $\chi^{(3)}$ is computed taking account of the Boltzmann distribution over vibrational–rotational levels, with the resonant in the IR-field part alone being essential:

$$\chi^{(3)} \approx \chi^{(3)}_{res} = \sum_v n_v \sum_j n_j \sum_{\Delta} \tilde{\chi}^{(3)}_{vj\Delta}\,, \tag{4}$$

where n_v is the relative population of the respective vibrational level, n_j is the relative population of the rotational sublevel, and the subscript Δ implies summation over different two-photon excitation channels (there are 9 such channels for the parallel band of symmetrical top molecules (Fig. 3)). Quantity

$$\tilde{\chi}^{(3)}_{vj\Delta} \propto \frac{d_{01}d_{12}}{\delta_{10}\delta_{20}}\,\alpha_{20}\beta_{20} \tag{5}$$

defines resonant cubic nonlinear susceptibility for a separate three-level system $|0\rangle - |1\rangle - |2\rangle$, shown in Fig. 3 with proper notations. The presence of two resonant factors in the denominator of the right-hand side of expression (5), namely, frequency detuning δ_{10} from one-photon resonance and detuning δ_{20} from two-photon resonance, makes the perturbation theory inapplicable for certain transitions when either $F_{01} \gtrsim |\delta_{10}|$ or $F_{01}F_{12} \gtrsim |\delta_{10}\delta_{20}|$, where quantities $F_{ij} = d_{ij}\mathcal{E}_{ir}/(2\hbar)$ are proportional to the amplitude of the strength of electrical component $\mathcal{E}_{ir}$ of the laser IR wave.[7] Going beyond the scope of the perturbation theory is effected by substitution $[2\pi/(c\hbar)^2]\, I_{ir}\tilde{\chi}^{(3)}_{vj\Delta} \to \rho_{02}$ in formulas (3)–(5), where ρ_{02} is the off-diagonal element of the density matrix describing IR field-induced polarization at the $|0\rangle - |2\rangle$ transition; hence, the following expression for the signal intensity of interest can be used:

$$I_{sum} = C|A|^2\,, \quad A = \sum_v n_v \sum_j n_j \sum_{\Delta} \rho_{02}\beta_{20}\,, \tag{6}$$

where factor L^2N^2, the intensity of visible radiation I_{vis}, and the vibrational component of Raman polarizability α_{20} are included in constant C. The nontrivial part of the I_{sum} intensity calculation is the calculation of quantities $\rho_{02}(\delta_{10}, \delta_{20}, F_{01}, F_{02})$ for each member of the sum in formula (6) with δ and F that, in turn, depend in some way on the quantum numbers of the respective states. The most important case is that in which parameters F of interaction between a molecule and the IR field essentially exceed the collisional width of vibrational–rotational lines. For this case, Ref. [12] offers the stationary solution of equations for the density matrix of a three-level system, leading to the expression

$$\begin{aligned}\rho_{02} \approx F_{01}F_{12}\big[&\delta_{10}\delta_{20}(\delta_{10}-\delta_{20})^2 + (\delta_{10}-\delta_{20})(\delta_{10}+2\delta_{20})\,F_{01}^2 \\ &- (\delta_{10}^2 - 6\delta_{10}\delta_{20} + \delta_{20}^2)\,F_{12}^2 + 2(F_{01}^2+F_{12}^2)(F_{01}^2-2F_{12}^2)\big] \\ &\times \big[\delta_{10}^2\delta_{20}^2(\delta_{10}-\delta_{20})^2 + 2\delta_{20}(\delta_{10}-\delta_{20}) \\ &\times (\delta_{10}^2 + 2\delta_{10}\delta_{20} - 2\delta_{20}^2)\,F_{01}^2 - 2\delta_{10}\delta_{20}(\delta_{10}^2 - 4\delta_{10}\delta_{20} + \delta_{20}^2) \\ &\times F_{12}^2 + (\delta_{10}^2 + 8\delta_{10}\delta_{20} - 8\delta_{20}^2)\,F_{01}^4 + 2(\delta_{10}^2 - \delta_{10}\delta_{20} + 10\delta_{20}^2) \\ &\times F_{01}^2F_{12}^2 + (\delta_{10}^2 - 10\delta_{10}\delta_{20} + \delta_{20}^2)\,F_{12}^4 + 4(F_{01}^2+F_{12}^2)^3\big]^{-1}\,. \end{aligned} \tag{7}$$

This theoretical description was applied to the CF_3Br gas. IR radiation is in quasiresonance with the mode ν_1 of the molecule. All important issues, such as the isotope composi-

[7] Transition dipole moments are expressed as the product of vibrational (d_{vib}) and rotational factors. Vibrational factors of the second and first transitions are related as $\sqrt{2}$ (oscillator law). Rotational factors depend in a certain way on the branch and three rotational quantum numbers [18].

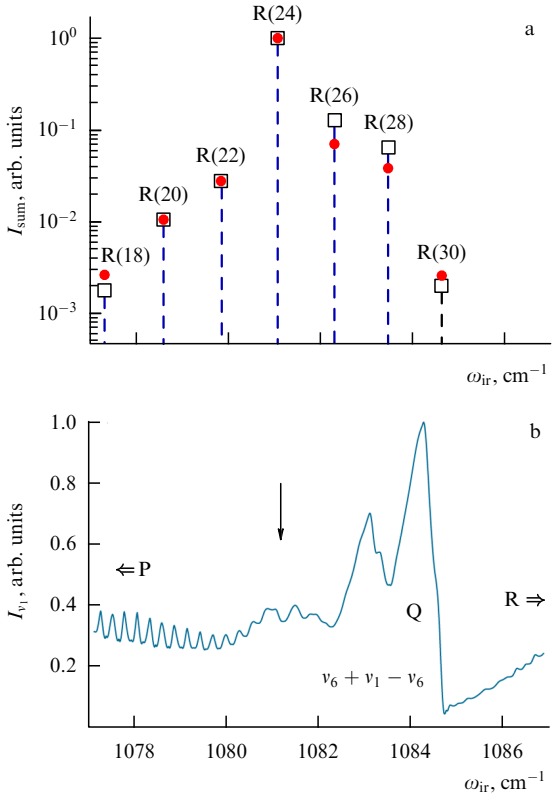

Figure 4. (a) Dependence of signal intensity I_{sum} at frequency $\omega_{sum} = 2\omega_{ir} + \omega_{vis}$ on IR-radiation frequency ω_{ir} in the v_1 band of the CF_3Br molecule. Experimental (squares) and theoretical (dots) data are shown with $F = d_{vib}\mathcal{E}_{ir}/(2\sqrt{3}\hbar) = 0.1$ cm^{-1} corresponding to experiment [12]. (b) Linear IR absorption spectrum at 300 K taken with a resolution of 0.1 cm^{-1}. Arrow indicates the position of the blue edge of the Q-branch of two-photon absorption for $CF_3{}^{81}Br$ (molecular content of 49.3%); isotopic shift for a lighter $CF_3{}^{79}Br$ molecule (50.7%) is 0.24 cm^{-1}.

Table 1. Contribution from rotational constituents of dipole moments and Raman polarizability to the amplitudes of different channels in four-wave frequency mixing $\omega_{sum} = 2\omega_{ir} + \omega_{vis}$ for the parallel band of a symmetrical top molecule.*

Parallel polarizations of IR and visible radiation		
Channel	*K*-dependence** with averaging over *M*	Averaging*** over *K*
PP, RR	$(1/30)\,(J^2 - K^2)^2/J^4$	4/225
PQ, QP, QR, RQ	$(1/15)(J^2 - K^2)\,K^2/J^4$	2/225
PR, RP	$(1/30)(2 - 3K^2/J^2 + K^4/J^4)$	9/225
QQ	$(1/15)(K^2/J^2 + 2K^4/J^4)$	11/225
Perpendicular polarizations of IR and visible radiation****		
Channel	*K*-dependence** in averaging over *M*	Averaging*** over *K*
PP, RR	$-(1/60)(J^2 - K^2)^2/J^4$	−2/225
PQ, QP, QR, RQ	$-(1/30)(J^2 - K^2)\,K^2/J^4$	−1/225
PR, RP	$(1/60)(3 - 2K^2/J^2 - K^4/J^4)$	8/225
QQ	$(1/15)(2K^2/J^2 - K^4/J^4)$	7/225

* Estimates for $J, K \gg 1$ with regard for the principal members alone. The data are presented only for the parallel constituent of vibrational Raman polarizability α_{20} predominant in the case of CF_3Br (see Ref. [12] for details).

** Normalization complies with the standard formulas for rotational components of transition dipole moments [18].

*** Rough estimate disregarding different populations of *K*-sublevels and *K*-dependence of δ_{10} and δ_{20} detunings.

**** This optimal experimental scheme with $\varphi = 90°$ is realized in Ref. [12] (see Fig. 3).

tion (in terms of bromine atoms), the choice of parameters in accordance with the experimental conditions, spectroscopic constants of the molecule, and the contribution from rotational components of dipole moments and Raman polarizability to the amplitudes of different channels, are described in Ref. [12]. A comparison of theoretical and experimental data for seven lines of the CO_2-laser is presented in Fig. 4a. The high sensitivity of the signal to the tuning of frequency ω_{ir} to the Q-branch of the two-photon transition observed in experiment is in excellent agreement with the theory.

The extreme difference between this dependence and the linear absorption spectrum presented in Fig. 4b should be emphasized. It has nothing in common with the fundamental band structure consisting not only of relatively narrow Q-branches of vibrational–rotational transitions from the ground and the first excited states of the lowest-frequency (doubly degenerate) mode $v_6 \approx 300$ cm^{-1}, but also of the not fully shown in the figure wide P-branch ($\Delta J = -1$) and R-branch ($\Delta J = +1$) integral absorption in which is practically the same as in the Q-branch. There are two reasons for such behavior. First, the spectrum practically lacks what is called 'nonresonant background' in four-wave mixing spectroscopy (e.g., as regards CARS) due to the presence of two quasiresonant transitions, i.e., relatively small frequency detunings δ_{10} and δ_{20} from one- and two-photon resonances [see explanation for formula (5)]. Second, rotational factors of products $d_{01}d_{02}\beta_{20}$ [see the diagram in Fig. 3 and formula (5)] dominate in three channels (those leading to two-photon transitions without a change in J (see Table 1 for relevant estimates and necessary comments).

To conclude this section, it is worthwhile to note the potentially important result presented in Fig. 4. As is known, applications of molecular spectroscopy to the analysis of molecular gases and their mixtures are based on the use of reference lines for individual molecules in IR and RS spectra. These are vibrational frequencies in low-resolution spectroscopy, and a full set of vibrational–rotational lines in different rotational branches in high-resolution spectroscopy. The overlap of vibrational bands of different mixture components inevitably makes difficult an analysis not infrequently involving the search for correlations in the measured spectrum [19].

It follows from the aforesaid that the spectroscopic technique that would yield, say, one line strongly distinguished in terms of intensity for each individual molecule within a vibrational band, could be very useful. The sum-frequency generation process with intermediate two-photon resonance has the desired spectral properties (at least for parallel bands of symmetrical top molecules). A thought experiment can be imagined in which broad-band IR radiation, e.g., produced by a parametric generator, is used together with narrow-band visible radiation utilized, in particular, for its pumping. Then, the spectrum of sum-

frequency generation will contain a narrow line at frequency $\omega_{20}+\omega_{\rm vis}$ in the case of a single-component gas or several lines in the case of a multi-component gas, the lines being readily resolved even if the linear absorption spectra of different components overlap.

However, whenever two isotopic modifications are present in the mixture, as in the case of CF_3Br, the possibility of their separate detection is dubious. It will be shown in Section 2.3 that the line R(24) of a CO_2-laser does not fall on the actual maximum of dependence $I_{\rm sum}(\omega_{\rm ir})$; in fact, the spectrum turns to be much narrower than can be expected: even the $CF_3{}^{79}Br$ and $CF_3{}^{81}Br$ lines spaced only 0.24 cm^{-1} apart, i.e., less than the Q-branch width, can be resolved.

2.2 Extremely narrow resonance inside the Q-branch of two-photon transition in the parallel band of symmetrical top molecule

The theoretical approach applied not only to discrete CO_2-laser frequencies, predicts [12] that continuous frequency tuning would give rise to two extremely sharp peaks approximately 0.08 cm^{-1} and 0.16 cm^{-1} apart from the R(24) line of the CO_2-laser towards the red and blue sides, respectively (for two isotopic modifications, $CF_3{}^{81}Br$ and $CF_3{}^{79}Br$, respectively), with the signal amplitude exceeding roughly by one order of magnitude that in experiment (see Fig. 5 presenting results of calculations for the monoisotopic $CF_3{}^{81}Br$ gas). Let us consider the $I_{\rm sum}(\omega_{\rm ir})$ dependence in the Q-branch of the two-photon transition to better understand the cause of the effect. The main contribution to the signal in this frequency region comes from three channels: PR $(J\to J-1\to J)$, QQ $(J\to J\to J)$, and RP $(J\to J+1\to J)$. Ignoring, for simplicity, the K-dependences of δ_{10} and δ_{20} leads for all three channels to

$$\delta_{20}=2\omega_{\rm ir}-2v-2x+(B_0-B_2)\,J(J+1)\,, \tag{8}$$

where v is the vibrational frequency, $x<0$ is the spectroscopic anharmonic constant, and B_0 and B_2 are the rotational constants in the $|v=0\rangle$ and $|v=2\rangle$ states, respectively. Detunings δ_{10} for various channels differ:

$$\begin{aligned}\delta_{10}^{\rm PR}&=\omega_{\rm ir}-v+2B_0J+(B_0-B_1)\,J(J-1)\,,\\ \delta_{10}^{\rm QQ}&=\omega_{\rm ir}-v+(B_0-B_1)\,J(J+1)\,,\\ \delta_{10}^{\rm RP}&=\omega_{\rm ir}-v-2B_0(J+1)+(B_0-B_1)(J+1)(J+2)\,,\end{aligned} \tag{9}$$

where B_1 is the rotational constant in the $|v=1\rangle$ state. It follows from Eqn (9) that in the QQ- and RP-channels at $\omega_{\rm ir}\simeq v+x$ (Q-branch of two-photon transition) one finds $\delta_{10}<0$ for all J, because $|B_0-B_1|\ll B_0$. Using formula (5) for orientation helps in understanding that the resonant in δ_{20} part of summation in formula (4) must not play an important role, because contributions to formula (5) from the levels with positive and negative δ_{20} are compensated for near resonance. The most important thing for sum (4) is contour asymmetry as a whole. Quantities $A^{\rm QQ}$ and $A^{\rm RP}$ pass maximum in modulus at the edges of the Q-branch for the two-photon transition and vanish somewhere in the center. The picture is different for the PR-channel. It follows from Eqn (8) and the first formula in Eqn (9) that a change in J alters the sign of both δ_{20} and δ_{10}. Taking again formulas (4) and (5) for orientation leads to the conclusion that $A^{\rm PR}$ amounts to a maximum at frequency $\tilde\omega_{\rm ir}$, near which δ_{10} and δ_{20} simultaneously change sign upon a change in J. The equality $B_0-B_2\approx 2(B_0-B_1)$ and inequality $|x|\gg B$ yield

$$\tilde\omega_{\rm ir}=v+\frac{B_0+B_1}{2B_1}\,x-\frac{B_0-B_1}{4B_1^2}\,x^2\,. \tag{10}$$

Dependence $A^{\rm PR}(\omega_{\rm ir})$ near the frequency $\tilde\omega_{\rm ir}$ can be estimated analytically using formula (7) in the $F_{01}\ll|\delta_{10}|$ approximation, i.e., assuming that single-photon resonance for the overwhelming majority of states in sum (4) can be considered in the framework of the perturbation theory. Then, it follows that

$$\rho_{02}\approx\frac{F_{01}F_{12}(\delta_{10}\delta_{20}+F_{01}^2-F_{12}^2)}{(\delta_{10}\delta_{20}+F_{01}^2-F_{12}^2)^2+4F_{01}^2F_{12}^2}\,, \tag{11}$$

where we can put $F_{01}=F_{12}/\sqrt{2}=F$ (oscillator law), and make use of formula (8) and the first formula in Eqn (9) in the explicit form. It is convenient to introduce the formally noninteger J_0 value resonant in the transition $|v=0\rangle\to|v=1\rangle$ for a given frequency $\omega_{\rm ir}$, replace summation in Eqn (6) by integration, and, since the main contribution to the integral comes from J, which satisfies inequality $|J-J_0|\ll J_0$, ignore the J-dependence of population, linearize expressions δ_{10} and δ_{20} with respect to $J-J_0$, and extend integration to infinite limits. Then, taking account of formula (11) leads to the expression

$$A^{\rm PR}\approx\frac{1}{6}\,\frac{\pi n(J_0)\,F}{\sqrt{(B_0-B_1)\,J_0\left[B_0(J_0+1)-B_1J_0\right]}}\,U(\varepsilon)\,, \tag{12}$$

where $n(J_0)$ is the relative population of states with $J\sim J_0$ and $U(\varepsilon)$ is the universal, normalized to unity at the maximum,

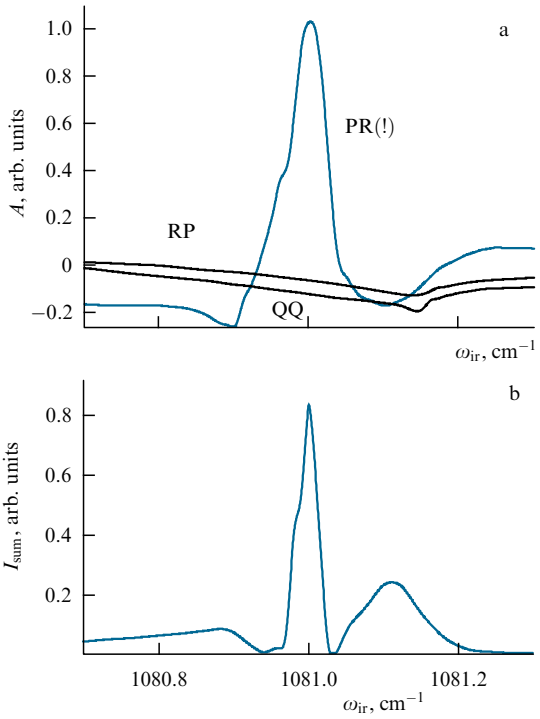

Figure 5. (a) Theoretical signal amplitudes in three channels in the narrow part of the $CF_3{}^{81}Br$ spectrum. (b) Respective signal intensity as the sum squared of the amplitudes for all nine channels. Initial data are the same as in figure (4a) comparing the results obtained by the theory and experiment.

function

$$U(\varepsilon) = \frac{3}{\sqrt{2}} \left\{ \frac{\left[(\varepsilon^2+1)^2+8\right]^{1/2} - (\varepsilon^2+1)}{(\varepsilon^2+1)^2+8} \right\}^{1/2} \qquad (13)$$

of the variable

$$\varepsilon = -\frac{x + 2B_1 J_0}{F} \left[\frac{B_0(J_0+1) - B_1 J_0}{2(B_0 - B_1)J_0} \right]^{1/2}, \qquad (14)$$

representing a contour with sharply ($\propto |\varepsilon|^{-3}$) falling wings and the full width at half-maximum (FWHM) $\Delta\varepsilon \approx 3$.

The above consideration explains the sharp peak in A^{PR} amplitude (Fig. 5a) and, as a consequence, in signal intensity (Fig. 5b) obtained by the exact calculation for the $CF_3{}^{81}Br$ molecule. Both the maximum position at $\varepsilon = 0$ or $\omega_{\mathrm{ir}} = \tilde{\omega}_{\mathrm{ir}}$ (which is practically the same) and the width of the contour A^{PR} are in excellent agreement with the results of computations upon substituting spectroscopic constants and the value of $\sqrt{3}F = d_{\mathrm{vib}}E_{\mathrm{ir}}/(2\hbar) = 0.1\ \mathrm{cm}^{-1}$ into formulas (12)–(14).

Experimental confirmation of the effect were possible a powerful enough laser with a continuously tunable the radiation frequency would be available. In a special case of CF_3Br gas, a reliable resolution of lines corresponding to isotopic species $CF_3{}^{79}Br$ (50.7%) and $CF_3{}^{81}Br$ (49.3%) could be expected. Because the isotopic shift is small ($0.24\ \mathrm{cm}^{-1}$), conventional linear spectroscopy permits the Q-branches of these two molecules to be resolved at very low rotational temperatures; therefore, monoisotopic gases are usually taken for spectroscopic studies (see, for instance, paper [20]).

2.3 Potential applications for diagnostics of intramolecular vibration redistribution

The intramolecular vibration redistribution (IVR) is a fundamental process taking place in an isolated polyatomic molecule at a reasonably high vibrational energy. This region of energies above a certain arbitrary boundary E_{onset} is related to the phenomenon known as dynamic chaos, common for systems with many degrees of freedom [21–27]. Important characteristics of dynamic chaos include the rates of IVR from different molecular modes. They are determined by laser methods of high spectral and temporal resolutions (see Refs [28–30] for a review). Process (1) can, in principle, be used in two variations: one with relatively long quasimonochromatic pulses, and the other with ultrashort pulses. Let us consider possible options using the example[8] analyzed in Sections 2.2. and 2.3 as a basis for estimation.

(1) The resonance width in Fig. 5 is roughly $0.05\ \mathrm{cm}^{-1}$, which is equivalent to $10^{10}\ \mathrm{s}^{-1}$. However, it cannot be smaller than the uniform width conditioned by the IVR effect, when the $v = 2$ level lies higher than energy E_{onset}. In other words, if the time of intramolecular vibration redistribution from the $|v = 2\rangle$ state is $\tau_{\mathrm{IVR}} \lesssim 10$ ps (as is actually the case for some molecular modes [33, 34]), it could result in an appreciable broadening of the resonance and consequently make possible the measurement of τ_{IVR}.

(2) The width of the Q-branch of two-photon transitions is roughly twice that of the Q-branch of a linear absorption, which suggests the standard value on the order of 1–2 cm^{-1} at room temperature (Fig. 4b). When $\tau_{\mathrm{IVR}} \lesssim 1$ ps, this time can, in principle, be measured in a pump–probe type experiment by exciting the $|v = 2\rangle$ state with a femtosecond IR laser pulse in resonance with two-photon transition $|v = 0\rangle \rightarrow |v = 2\rangle$ and probing with a femtosecond optical laser pulse controllably delayed with respect to the pump pulse. The τ_{IVR} value is then estimated from a decrease in intensity of directed coherent radiation at frequencies $\omega_{\mathrm{sum}} \approx \omega_{20} + \omega_{\mathrm{vis}}$. It should be noted that a positive result can be obtained at longer IVR time only by severely narrowing the Q-branch with the aid of a cooled molecular beam, because the negative factor is the dephasing of off-diagonal elements ρ_{02} of the density matrix for states with different rotational quantum numbers, so that the dephasing time is on the order of the Q-branch inverse width.

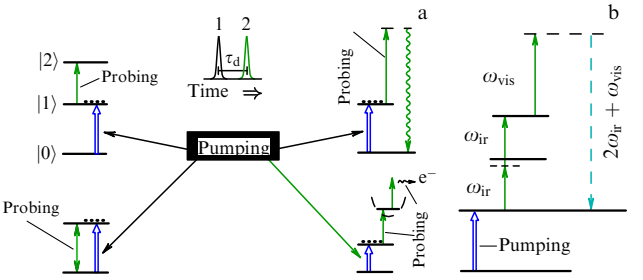

Figure 6. Schematics of different experiments for the real-time study of the IVR process. The signal is proportional to the population of level $|v = 1\rangle$. IVR dynamics is diagnosed by the dependence of the signal on delay time τ_{d} of probing laser pulse 2 relative to pulse 1 exciting the transition $|v = 0\rangle \rightarrow |v = 1\rangle$. (a) Approved schemes (see the text). (b) Probing scheme (see the text) based on sum-frequency generation with intermediate two-photon resonance.

(3) Process (1) can be applied to probe the population of the $|v = 1\rangle$ state during IVR from this state. Such an approach is, in principle, analogous to other approved pump–probe methods for real time IVR studies in individual molecules. Four such schemes are presented in Fig. 6a (clockwise from the top left corner): (1) based on IR absorption in the $|v = 1\rangle \rightarrow |v = 2\rangle$ transition [35]; (2) based on anti-Stokes RS in the $|v = 1\rangle \rightarrow |v = 0\rangle$ transition [36–40]; (3) based on photoionization from the $|v = 1\rangle$ state [33, 41--43], and (4) based on induced bleaching in the $|v = 0\rangle \leftrightarrow |v = 1\rangle$ transition [34, 44–47]. A comparative analysis of the advantages and disadvantages of these approaches is presented in review [30]. It should be noted that the most readily interpretable method based on the employment of anti-Stokes RS has two drawbacks, namely a weak signal and the impossibility of working in the subpicosecond range due to strong background luminescence caused by multiphoton processes. Therefore, it is highly desirable to take advantage of a much intense coherent process instead of RS. The scheme in Fig. 6b explains how process (1) can be employed for this purpose. It is assumed that the state $|v = 1\rangle$ of the high-frequency mode is above energy E_{onset}. The frequency of the probing IR laser is tuned to the Q-branch of the two-photon transition $|v = 1\rangle \rightarrow |v = 3\rangle$. The time of IVR from the state $|v = 1\rangle$ will be estimated from the decay of coherent radiation at the sum-frequency. Potential complication arises from the fact that the IR laser spectrum can overlap the two-photon transition $|v = 0\rangle \rightarrow |v = 2\rangle$. However, all other conditions being equal, coherent radiation intensity with the initial state

[8] To recall, the E_{onset} boundary in a CF_3Br molecule is estimated approximately at 7500 cm^{-1} [31, 32], which is much higher than the energy of state $|v = 2\rangle$ of the ν_1 mode. Therefore, this is a purely speculative example as far as IVR is concerned.

$|v = 1\rangle$ normalized to the population squared is three times more than with the initial state $|v = 0\rangle$. Therefore, the ratio of the useful signal to the background would be acceptable for qualitative measurements, e.g., the 1:3 ratio is achieved upon excitation of 25% of the molecules by the first laser pulse.

3. Two-photon spectroscopy of Raman-active mode

Let us discuss Ref. [1], published in *Physical Review Letters*, which encouraged us to write the present article. The study subject was the CH_4 molecule (methane). The classification and vibrational frequencies of this molecule are presented in Fig. 7. The totally symmetric mode ν_1 is active only with respect to the RS process. Its spectrum can be more effectively investigated applying CARS (Fig. 1a) than the spontaneous variant. For example, Ref. [49] reported measurements of the high-resolution spectrum of the ν_1 mode Q-branch in a molecular beam cooled to 31.5 K. The authors of Ref. [1] proposed a variant of four-wave mixing with a novelty element as regards CARS, consisting in the fact that coherence in transition $|g\rangle \leftrightarrow |v_1 = 1\rangle$ is produced by a *single* IR-laser, the double frequency of which is close to ν_1, rather than by *two* visible-light lasers with the frequency difference tuned in the vicinity of ν_1. It is a seemingly insignificant distinction, but the two-photon transition involves here the intermediate level (Fig. 2b), namely, the first excited state of the IR-active mode ν_4. The authors of Ref. [1] argued that the

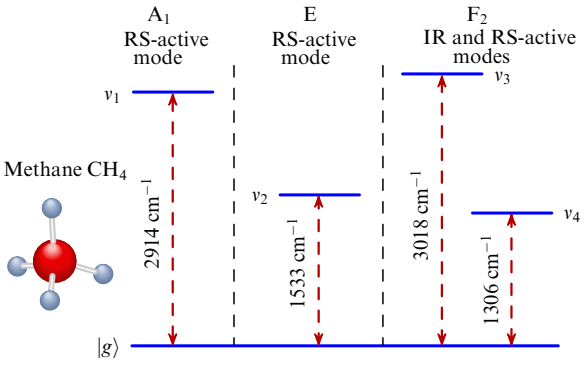

Figure 7. Nine vibrational degrees of freedom of CH_4 molecule include four modes [48]: nondegenerate mode ν_1 of A_1 symmetry, doubly degenerate ν_2 of E symmetry, and triply degenerate ν_3 and ν_4 of F_2 symmetry. Two modes are active only in RS, and two others in both IR-absorption and RS.

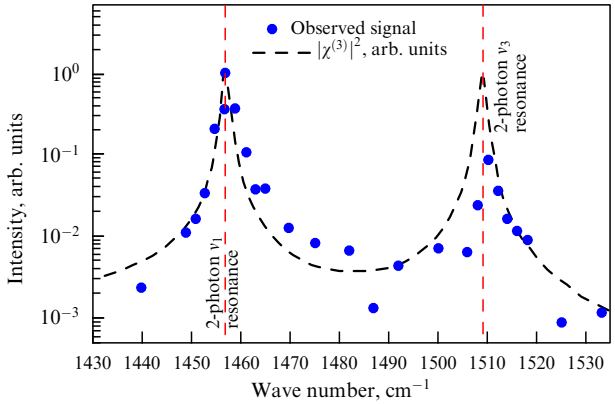

Figure 8. Methane (CH_4) molecule. Dependence of intensity of coherent radiation at sum frequency $\omega_{sum} = 2\omega_{ir} + \omega_{vis}$ on IR-laser frequency ω_{ir}. Experimental (dots) and theoretical (curve) data. (Taken from Ref. [1].)

relative proximity of this state to frequency ω_{ir} must enhance the efficiency of the process over that of CARS and markedly suppress the nonresonant background (the explanation in this case is analogous to that in Section 2).

The result of the experiment is presented in Fig. 8. The frequency of the IR-laser was tuned within the range $\Delta\omega_{ir} \sim 100$ cm^{-1}. The peaks at frequencies of 1457 cm^{-1} and 1509 cm^{-1} corresponded to two-photon resonances in transitions $|g\rangle \to |v_1 = 1\rangle$ and $|g\rangle \to |v_3 = 1\rangle$, respectively. The nonresonant background was actually suppressed. Also, good agreement between theory and experiment was achieved. As far as higher efficiency than that of CARS is concerned, the authors claimed only that at the maximum laser pulse energy the sum-frequency signal (1) was 500 times stronger than the spontaneous RS signal, but any comparison with CARS was not presented. The latter is surprising, since separate lines of the Q-branch in the ν_1 band have been resolved in an earlier study [49] with the aid of a continuous Ar^+-laser and a tunable dye laser pumped by it.

For completeness, let us compare technical details of experiments [1] and [12]. Parameters of the laser pulses used in both papers are presented in Table 2. Despite their different lengths in the two experiments, 'rough' spectral features are virtually identical; specifically, the signal is highly sensitive to the tuning to the Q-branch of the two-photon transition.

It should also be noted that the efficiencies of the two schemes are not principally different. Indeed, both include a single weak transition (see the last line in Table 2): the

Table 2. Comparison of selected characteristics of experiments [1] and [12] on the generation of sum frequency $\omega_{sum} = 2\omega_{ir} + \omega_{vis}$.

Characteristic	Experiment [1]	Experiment [12]
IR-laser Pulse energy and duration Line width	Optical parametric oscillator* 6 μJ, 30 ps Not specified***	CO_2-laser Maximum energy** $\lesssim$1 J, 80–300 ns 0.03 cm^{-1}
Visible-range laser Pulse energy and duration	Nd:YAG, 2nd harmonic (532 nm) 330 μJ, 30 ps	Nd:YAG, 2nd harmonic (532 nm) 40 mJ, 10 ns
'Weak' transition	$\|v_4 = 1\rangle \to \|v_1 = 1\rangle$, IR difference band	$\|v = 2\rangle \to \|v = 0\rangle$, overtone RS transition

* Focusing was used, but energy fluence not specified.
** Energy fluences of 30–50 mJ cm^{-2} were actually used.
*** Judging by the size of experimental points, the line width was $\sim$ 1 cm^{-1}.

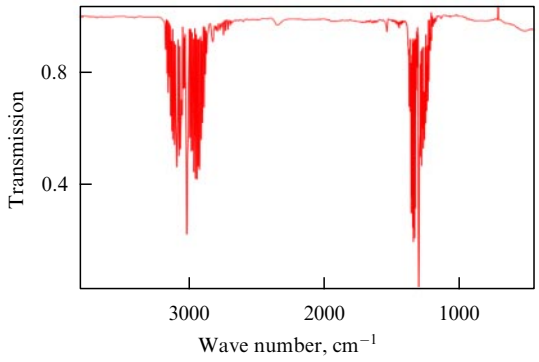

Figure 9. Transmission spectrum of CH_4 molecule at room temperature and 150 mm Hg in a mixture with nitrogen at 450 mm Hg. Resolution is 4 cm^{-1}. (Source — NIST Chemistry WebBook, https://webbook.nist.gov/chemistry.)

difference IR band for the scheme in Fig. 2b and the overtone RS band for that in Fig. 2a, but the relative weakness of these two transitions within the framework of the Born–Oppenheimer approximation [50] is identical.

From the point of view of potential applications, weakness of the scheme oriented to 'accidental' intermediate resonance (Fig. 2b) comes from its nonuniversality. Another drawback is that this scheme is hardly suitable for observing the narrow resonance predicted theoretically in Section 2.2, because it is unlikely that intermediate quasiresonance would fall within an absorption band. Thus, in the case of the methane molecule the frequency of the IR-active mode v_4 (see Fig. 7) differs by -151 cm^{-1} from the half-frequency of v_1 and by -203 cm^{-1} from the half-frequency of v_3, whereas the half-width of the band at the baseline toward the shorter wavelengths is only 70 cm^{-1} (Fig. 9).

At the same time, there is an important advantage: the possibility of two-photon spectroscopy of the RS-active mode in a molecule with a center of symmetry for which IR-transitions are forbidden. This potentiality may be of special importance for measuring the IVR rate from excited states of RS-active modes. The actual examples are the molecules as exemplified by C_6H_6, $W(CO)_6$, and $Cr(CO)_6$ molecules, for which the IVR process from IR-active modes was studied in Refs [51, 52], [44, 45], and [34], respectively. Essentially the same methods as those considered in Section 2.3 are applied to studying IVR from RS-active modes.

4. Conclusions

We explored two publications to demonstrate a broad potential applications of nonlinear coherent spectroscopy, making possible much more selective identification of molecules than linear spectroscopic techniques due to the extremely high sensitivity of signal intensity to the tuning of an IR-laser to the Q-branch of the two-photon transition. Reference [12] was the first systematic study of this resonance property of certain spherical and symmetrical top molecules. A new result for such molecules (and also for spherical tops) has recently been reported in paper [1]. The authors of this work concluded their paper by the assertion that possible useful applications of the method in question include "molecular gas detection in environmental applications as well as chemical-specific imaging in microscope." We would like to emphasize in more details the physical applications, such as providing molecules with ultranarrow reference lines (see Section 2.2) and the potentialities for studies of the intramolecular vibration redistribution process (see Section 2.3).

Spectroscopic capabilities of the method can be expanded by utilizing two IR-laser frequencies. In this case a narrow resonance with a width of order $d_{\rm vib}E_{\rm ir}/(2\hbar)$ will be observed naturally upon frequency tuning to Q-lines of one-photon transitions $0-1$ and $1-2$ corresponding to the same J. Another interesting option of sum-frequency $\omega_{\rm sum} = \omega_{\rm mw} + \omega_{\rm ir} + \omega_{\rm vis}$ generation is that in which a microwave, purely rotational, transition with a given J takes place at the first step. However, the use of such 'three-frequency' schemes — much more complicated than 'two-frequency' schemes — is justified only by a specific character of a problem, e.g., when rotational state selectivity is needed.

In our opinion, the most substantial circumstance responsible for the more than 30-year delay in implementing the method in coherent laser molecular spectroscopy was the absence of powerful enough narrow-linewidth IR-lasers that, in addition, are continuously turnable and frequency stable. The high-pressure CO_2-laser, which was created in the 1970s [53–55], proved highly 'capricious', even as a prototype instrument. We are unaware of its application for spectroscopic measurements in any laboratory in this or other countries. Meanwhile, such a laser combining high power and narrow linewidth would be an ideal device for spectroscopy in the 9–11-μm wavelength range. Optical parametric oscillators, such as the one employed in Ref. [1], have actually no alternative to date.[9] The efforts of scientists must be directed first and foremost toward considerably narrowing the linewidth to enable the observation of ultranarrow resonances (see Fig. 5) conditioned by the simultaneous contribution from many rotational states. It should be noted that laser intensity is also important for the manifestation of accidental two-photon resonances at individual vibrational–rotational two-photon transitions only as minor occasional fluctuations.[10] It was mentioned in the foregoing that this effect can be observed with the use of a continuously tunable IR-laser. The presence of narrow resonance is of consequence for those applications of molecular spectroscopy that require resolution of the spectra of mixture components with overlapping IR-absorption bands or overlapping bands differing in the initial vibrational states of a molecule (this problem arises in the study of nonstationary vibrational dynamics of molecules, e.g., in the case of cooling in supersonic jets or multiphoton excitation of molecules by IR-laser radiation).

The results available thus far are largely related to spherical tops and parallel bands of symmetrical top molecules. The sole exception is the BCl_3 molecule, for which the perpendicular band (the two-fold degenerate v_3 mode) was examined [12]. In this case, a strongly distinguished signal was registered on three adjacent lines of the CO_2-laser. Without detailed calculations, it is difficult to say whether there is here a well-defined resonant structure. Therefore, it can be predicted that calculations of the effects

[9] It can be expected that quantum cascade lasers will provide one more adequate (in terms of parameters) tool in the near future (see paper [56]).
[10] The rapidly developing technique based on optical parametric amplification of powerful laser systems producing ultrashort pulses in the mid-infrared range will possibly greatly contribute to the solution of the problems at hand (see review [57]).

of sum-frequency generation with intermediate two-photon resonance for perpendicular bands of symmetric tops and different bands of asymmetric tops based on precision determination of spectroscopic constants would be highly opportune.

References

1. Traverso A J et al. *Phys. Rev. Lett.* **120** 063602 (2018)
2. Akhmanov S A, Koroteev N I *Sov. Phys. Usp.* **20** 899 (1977); *Usp. Fiz. Nauk* **123** 405 (1977)
3. Akhmanov S A, Koroteev N I *Metody Nelineinoi Optiki v Spektroskopii Rasseyaniya Sveta* (Methods of Nonlinear Optics in Scattered Light Spectroscopy) (Moscow: Nauka, 1981)
4. Akhmanov S A, in *Nonlinear Spectroscopy* (Ed. N Bloembergen) (Amsterdam: North Holland, 1977) Ch. 9; Translated into Russian: in *Nelineinaya Spektroskopiya* (Ed. N Bloembergen) (Moscow: Mir, 1979) p. 267
5. Kildal H, Brueck S R J *Phys. Rev. Lett.* **38** 347 (1977)
6. Kung R T V, Many S A *Appl. Phys.* **50** 2548 (1979)
7. Akhmanov S A et al. *Pis'ma Zh. Tekh. Fiz.* **5** 1507 (1979)
8. Chung K M, Stevens G, Becker M F *IEEE J. Quantum Electron.* **15** 874 (1979)
9. Yevseyev I V, Rubtsova N N, Samartsev V V *Kogerentnye Perekhodnye Protsessy v Optike* (Coherent Transient Processes in Optics) (Moscow: Fizmatlit, 2009) Ch. 2
10. Zel'dovich B Ya, Pilipetskii N F, Shkunov V V *Sov. Phys. Usp.* **25** 713 (1982); *Usp. Fiz. Nauk* **138** 249 (1982)
11. Letokhov V S, Chebotaev V P *Nelineinaya Lazernaya Spektroskopiya Sverkhvysokogo Razresheniya* (Nonlinear Laser Spectroscopy of Ultrahigh Resolution) (Moscow: Nauka, 1990) Ch. 6
12. Dolzhikov V S et al. *Sov. J. Quantum Electron.* **16** 580 (1986); *Kvantovaya Elektron.* **13** 887 (1986)
13. Pellin M J, Yardley J T *Appl. Phys. Lett.* **29** 304 (1976)
14. Akhmanov S A *Sov. J. Quantum Electron.* **6** 1012 (1976); *Kvantovaya Elektron.* **3** 1846 (1976)
15. Varakin V N, Gordienko V M, Lopatin A F, Preprint No. 3 (Moscow: Faculty of Physics, Lomonosov Moscow State Univ., 1981)
16. Varakin V N, Gordienko V M, in *Trudy VII Vavilovskoi Konf. po Nelineinoi Optike, Iyun' 1981 g.* (Proc. of the VII Vavilov Conf. on Nonlinear Optics, June 1981) Pt. 2 (Ed. S G Rautian) (Novosibirsk: Institut Avtomatiki i Elektrometrii SO AN SSSR, 1982) p. 214
17. Zheltikov A M, Koroteev N I *Phys. Usp.* **42** 321 (1999); *Usp. Fiz. Nauk* **169** 385 (1999)
18. di Lauro C, Mills I M *J. Mol. Spectrosc.* **21** 386 (1966)
19. Smith A L *Applied Infrared Spectroscopy*: *Fundamentals, Techniques, and Analytical Problem-Solving* (Chemical Analysis, Vol. 54) (New York: Wiley, 1979); Translated into Russian: *Prikladnaya IK-Spektroskopiya*: *Osnovy, Tekhnika, Analiticheskoe Primenenie* (Moscow: Mir, 1982)
20. Bürger H, Burczyk K, Schulz P *Spectrochim. Acta A* **38** 627 (1982)
21. Zaslavskii G M, Chirikov B V *Sov. Phys. Usp.* **14** 549 (1972); *Usp. Fiz. Nauk* **105** 3 (1971)
22. Gaponov-Grekhov A V, Rabinovich M I *Sov. Phys. Usp.* **22** 590 (1979); *Usp. Fiz. Nauk* **128** 579 (1979)
23. Chirikov B V *Phys. Rep.* **52** 265 (1979)
24. Lichtenberg A J, Liberman M A *Regular and Stochastic Motion* (New York: Springer, 1983); Translated into Russian: *Regulyarnaya i Stokhasticheskaya Dinamika* (Moscow: Mir, 1984)
25. Zaslavsky G M *Chaos in Dynamic Systems* (New York: Harwood Acad. Publ., 1985); Translated from Russian: *Stokhastichnost' Dinamicheskikh Sistem* (Moscow: Nauka, 1984)
26. Gutzwiller M C *Chaos in Classical and Quantum Mechanics* (New York: Springer, 1990)
27. Ott E *Chaos in Dynamical Systems* (New York: Cambridge Univ. Press, 1993)
28. Lehmann K K, Scoles G, Pate B H *Annu. Rev. Phys. Chem.* **45** 241 (1994)
29. Nesbitt D J, Field R W *J. Phys. Chem.* **100** 12735 (1996)
30. Makarov A A, Malinovsky A L, Ryabov E A *Phys. Usp.* **55** 977 (2012); *Usp. Fiz. Nauk* **182** 1047 (2012);
31. Doljikov Yu S et al. *Chem. Phys. Lett.* **124** 304 (1986)
32. Dolzhikov Yu S et al. *Sov. Phys. JETP* **63** 1161 (1986); *Zh. Eksp. Teor. Fiz.* **90** 1982 (1986)
33. Yamada Y et al. *J. Chem. Phys.* **120** 7400 (2004)
34. Chekalin S V et al. *J. Phys. Chem. A* **118** 955 (2014)
35. Yoo H S, DeWitt M J, Pate B H *J. Phys. Chem. A* **108** 1348 (2004)
36. Malinovsky A L, Makarov A A, Ryabov E A *JETP Lett.* **80** 532 (2004); *Pis'ma Zh. Eksp. Teor. Fiz.* **80** 605 (2004)
37. Malinovsky A L et al. *Chem. Phys. Lett.* **419** 511 (2006)
38. Malinovsky A L, Makarov A A, Ryabov E A *JETP* **106** 34 (2006); *Zh. Eksp. Teor. Fiz.* **133** 45 (2006)
39. Makarov A A, Malinovsky A L, Ryabov E A *J. Chem. Phys.* **129** 116102 (2008)
40. Malinovsky A L, Makarov A A, Ryabov E A *JETP Lett.* **93** 124 (2011); *Pis'ma Zh. Eksp. Teor. Fiz.* **93** 139 (2011)
41. Ebata T et al. *J. Phys. Chem. A* **105** 8623 (2001)
42. Yamada Y, Mikami N, Ebata T *J. Chem. Phys.* **121** 11530 (2004)
43. Yamada Y et al. *J. Chem. Phys.* **123** 124316 (2005)
44. Myers D J et al. *Chem. Phys. Lett.* **312** 399 (1999)
45. Stromberg C, Myers D J, Fayer M D *J. Chem. Phys.* **116** 3540 (2002)
46. Kompanets V O et al. *JETP Lett.* **92** 135 (2010); *Pis'ma Zh. Eksp. Teor. Fiz.* **92** 157 (2010)
47. Chekalin S V et al. *Chem. Phys. Lett.* **512** 178 (2011)
48. Landau L D, Lifshitz E M *Quantum Mechanics*: *Non-Relativistic Theory* (Oxford: Pergamon Press, 1965); Translated from Russian *Kvantovaya Mekhanika. Nerelyativistskaya Teoriya* (Moscow: Fizmatlit, 1963) p. 440
49. Gustafson E K, McDaniel J C, Byer L R *Opt. Lett.* **7** 434 (1982)
50. Born M, Oppenheimer R *Ann. Physik* **84** 457 (1927)
51. Page R H, Shen Y R, Lee Y T *Phys. Rev. Lett.* **59** 1293 (1987)
52. Page R H, Shen Y R, Lee Y T *J. Chem. Phys.* **88** 4621 (1988)
53. Bagratashvili V N et al. *Opt. Commun.* **9** 135 (1973)
54. Bagratashvili V N, Knyazev I N, Lobko V V *Sov. J. Quantum Electron.* **5** 857 (1975); *Kvantovaya Elektron.* **2** 1577 (1975)
55. Bagratashvili V N et al. *Sov. J. Quantum Electron.* **6** 541 (1976); *Kvantovaya Elektron.* **3** 1011 (1976)
56. Vitiello S M et al. *Opt. Express* **23** 5167 (2015)
57. Mitrofanov A V et al. *Phys. Usp.* **58** 89 (2015); *Usp. Fiz. Nauk* **185** 97 (2015)